JOURNAL OF BACTERIOLOGY, Oct. 2002, p. 5706–5713 Vol. 184, No. 20
0021-9193/02/$04.00+0 DOI: 10.1128/JB.184.20.5706–5713.2002

Genes Encoding Specific Nickel Transport Systems Flank the Chromosomal Urease Locus of Pathogenic Yersiniae

Florent Sebbane,[1] Marie-Andrée Mandrand-Berthelot,[2] and Michel Simonet[1]*

Equipe Inserm E9919-Université JE2225-Institut Pasteur de Lille, Département de Pathogenèse des Maladies Infectieuses, Institut de Biologie de Lille, F-59021 Lille,[1] and Unité de Microbiologie et Génétique, Composante INSA, UMR 5122 CNRS-UCB-INSA, F-69622 Villeurbanne,[2] France

Received 16 April 2002/Accepted 18 July 2002

The transition metal nickel is an essential cofactor for a number of bacterial enzymes, one of which is urease. Prior to its incorporation into metalloenzyme active sites, nickel must be imported into the cell. Here, we report identification of two loci corresponding to nickel-specific transport systems in the gram-negative, ureolytic bacterium *Yersinia pseudotuberculosis*. The loci are located on each side of the chromosomal urease gene cluster *ureABCEFGD* and have the same orientation as the latter. The *yntABCDE* locus upstream of the *ure* genes encodes five predicted products with sequence homology to ATP-binding cassette nickel permeases present in several gram-negative bacteria. The *ureH* gene, located downstream of *ure*, encodes a single-component carrier which displays homology to polypeptides of the nickel-cobalt transporter family. Transporters with homology to these two classes are also present (again in proximity to the urease locus) in the other two pathogenic yersiniae, *Y. pestis* and *Y. enterocolitica*. An *Escherichia coli nikA* insertion mutant recovered nickel uptake ability following heterologous complementation with either the *ynt* or the *ureH* plasmid-borne gene of *Y. pseudotuberculosis*, demonstrating that each carrier is necessary and sufficient for nickel transport. Deletion of *ynt* in *Y. pseudotuberculosis* almost completely abolished bacterial urease activity, whereas deletion of *ureH* had no effect. Nevertheless, rates of nickel transport were significantly altered in both *ynt* and *ureH* mutants. Furthermore, the *ynt ureH* double mutant was totally devoid of nickel uptake ability, thus indicating that Ynt and UreH constitute the only routes for nickel entry. Both Ynt and UreH show selectivity for Ni^{2+} ions. This is the first reported identification of genes coding for both kinds of nickel-specific permeases situated adjacent to the urease gene cluster in the genome of a microorganism.

Urease, produced by a wide range of eukaryotic and prokaryotic organisms, is an enzyme that hydrolyzes urea to give ammonia and carbamate. This multimeric enzyme requires nickel for activity and is thus classed as a metalloenzyme (23). Bacteria have devised elaborate mechanisms for acquisition and incorporation of the divalent nickel ion. Nickel uptake constitutes the first step in this process. Diffusion of cations through the outer membrane of gram-negative bacteria occurs preferentially via the OmpC and OmpF porins (25). Translocation of nickel through the cytoplasmic membrane is then mediated by the nonspecific CorA and Mgt magnesium transport systems (33) and/or high-affinity, nickel-specific permeases (12). To date, two classes of high-affinity nickel transporters have been described for bacteria. The first, the Nik system, was originally identified as being essential for hydrogenase activity in *Escherichia coli* and is a member of the ATP-binding cassette (ABC) family. It consists of five components: a periplasmic binding protein (NikA) exhibiting high specificity for nickel, two integral cytoplasmic membrane proteins (NikB and NikC) assumed to form a channel for nickel transport, and finally, two membrane-associated ATPases (NikD and NikE) which are responsible for coupling energy to the transport process (24). Expression of the *E. coli nik* operon is activated (in the absence of oxygen) by the global regulatory protein FNR and repressed (in the presence of high nickel concentrations) by the nickel-responsive regulator NikR, which is functionally similar to the Fur ferric ion uptake regulator (5, 8, 39). Similar ABC transport systems with significant homology to the *E. coli* Nik proteins have recently been described for two human pathogens, *Vibrio parahaemolyticus* (26) and *Brucella suis* (18).

The second type of nickel importer is a single-component permease; the prototype of this class is HoxN from *Ralstonia eutropha* (previously *Alcaligenes eutrophus*). HoxN is an integral protein containing eight membrane-spanning segments (13). Members of this family have been identified in a number of bacteria, including *Helicobacter pylori* (22), *Bradyrhizobium japonicum* (14), and *Mycobacterium tuberculosis* (6), as well as in the fission yeast, *Schizosaccharomyces pombe* (11). Mutations in either specific transport system lead to a dramatic reduction in bacterial nickel uptake and, consequently, to decreased activity of the relevant nickel-requiring urease and hydrogenase enzymes (12, 17, 24).

The gram-negative enteropathogenic bacterium *Yersinia pseudotuberculosis* is a ureolytic species responsible for self-limiting, intestinal tract infections in humans. Genes involved in urease biosynthesis have recently been characterized (28). Three adjacent chromosomal genes (*ureA*, *ureB*, and *ureC*) encode the structural subunits which associate to constitute an inactive apoenzyme. Incorporation of nickel ions into the enzyme's catalytic site (located in the UreC protein) requires at least four additional genes (*ureE*, *ureF*, *ureG*, and *ureD*, situated in that order on the chromosome) contiguous to the

* Corresponding author. Mailing address: Département de Pathogenèse des Maladies Infectieuses, Institut de Biologie de Lille, 1, rue du Professeur Calmette, F-59021 Lille Cedex, France. Phone: 33 3 20 87 11 78. Fax: 33 3 20 87 11 83. E-mail: michel.simonet@ibl.fr.

TABLE 1. Strains and plasmids used in this study

Strain or plasmid	Relevant property(ies)[a]	Reference or origin
Strains		
Yersinia pseudotuberculosis		
32777	Wild-type strain	28
MYUH	Derived from strain 32777, Δ*ureH*Ω*aphA-1a*	This work
MYNT	Derived from strain 32777, Δ*yntABCDE*Ω*cat*	This work
MYOU	Derived from strain 32777, Δ*yntABCDE*Ω*cat* Δ*ureH*Ω*aphA-1a*	This work
Escherichia coli		
DH5α	*supE* Δ*lacU169* (ϕ80d*lacZ*Δ*M15*) *thi deoR phoA hsdR recA endA gyrA relA*	16
SY327λ*pir*	Δ(*lac pro*) *argE*(Am) *recA rif nalA* λ*pir*; host for pCVD442 and derivatives	21
SM10λ*pir*	*thi thr leu sup tonA lacY recA*::RP4-2Tc::MuKm λ*pir;* host for pCVD442 and derivatives	32
P4X	Hfr *metB*	24
HPX72	Derived from strain P4X, *nikA*::MudI (Km *lac*)	24
Plasmids		
pZero2-1	Cloning vector, Km	Invitrogen
pUC18	Cloning vector, Ap	36
pACYC184	Plasmid vector, Cm Tc; source of the chloramphenicol acetyltransferase *cat* gene	4
pUC4K	Plasmid vector; Km; source of the aminoglycoside phosphotransferase *aphA-1a* gene	34
pCVD442	Suicide vector containing the counterselectable marker *sacB*; Ap	9
pMS89	pHC79Ω, ~35-kb *Sau*3A DNA fragment from *Y. pseudotuberculosis* 32777 containing the urease locus and its flanking regions	28
pLW21	pUC19Ω, 7.1-kb *Sma*I insert with the *nikABCDER* region from *E. coli* K-12	24
pFS45	pUC18Ω, ~2.4-kb *Xho*I/*Bst*1107I insert with the 3′ end of *yut* and *ureH* from *Y. pseudotuberculosis* 32777	This work
pFS50	pACYC184Ω, ~7.3-kb *Hin*dIII/*Pst*I insert with the *Y. pseudotuberculosis* 32777 *ure* locus and its promoter region	This work
pFS78	pUC18Ω, ~5.5-kb PCR-generated fragment with primer set N1-N13 containing *ynt* genes from *Y. pseudotuberculosis* 32777	This work
pFSU1	pZero2-1Ω, ~1.2-kb *Xba*I/*Eco*RI PCR-generated fragment with primer set N5-N6 encompassing the upstream region of *ureH* gene from *Y. pseudotuberculosis* 32777	This work
pFSU2	pFSU1Ω, ~0.8-kb *Sac*I/*Eco*RI PCR-generated fragment with primer set N7-N8 encompassing the downstream region of *ureH* gene from *Y. pseudotuberculosis* 32777	This work
pFSU3	pFSU2Ω, ~1.3-kb *Eco*RI PCR-generated fragment with primer set K1-K2 encompassing *aphA-1a* from pUC4K	This work
pFSΔU	pCVD442Ω, ~3.3-kb *Xba*I/*Sac*I insert from pFSU3	This work
pFSO1	pUC18Ω, ~0.5-kb *Hin*dIII/*Pst*I PCR-generated fragment with primer set N1-N2 encompassing the upstream region of *yntA* gene from *Y. pseudotuberculosis* 32777	This work
pFSO2	pFSO1Ω, ~0.5-kb *Bam*HI/*Eco*RI PCR-generated fragment with primer set N3-N4 encompassing the downstream region of *yntE* gene from *Y. pseudotuberculosis* 32777	This work
pFSO3	pFSO2Ω, ~1.4-kb *Pst*I/*Bam*HI PCR-generated fragment with primer set C3-C4 encompassing the *cat* gene from pACYC184	This work
pFSΔO	pCVD442Ω, ~2.4-kb *Sac*I insert from pFSO3	This work

[a] Ap, Cm, Km, and Tc, resistance to ampicillin, chloramphenicol, kanamycin, and tetracycline, respectively. Ω, in vitro insertion.

structural genes. In this report, we show that *Y. pseudotuberculosis* produces two different types of specific nickel transporters (the synthesis of which is mediated by genes flanking the 5′ and 3′ ends of the *ure* locus): a multicomponent ABC nickel transporter encoded by the *yntABCDE* locus and located upstream of *ure* and a single-component transporter encoded by the *ureH* gene and located downstream of *ure*.

MATERIALS AND METHODS

Bacterial strains, plasmids, and growth conditions. The main characteristics of the bacterial strains and plasmids used in this study are listed in Table 1. *Y. pseudotuberculosis* and *E. coli* strains were grown at 28 and 37°C, respectively, in Luria-Bertani (LB) broth or on agar plates. Mating experiments were carried out by plating on M9 minimum medium agar (33 mM Na_2HPO_4, 22 mM KH_2PO_4, 8.5 mM NaCl, 18 mM NH_4Cl, 1 mM $MgSO_4$, 0.1 mM $CaCl_2$, 0.3 μM thiamine, 10 mM glucose, 14 g of agar/liter). Ampicillin (100 μg ml^{-1}), kanamycin (50 μg ml^{-1}), and chloramphenicol (50 μg ml^{-1}) were added to growth media for bacterial selection when necessary.

Yersinia and *Escherichia* strains were characterized with API 20E strips (bioMérieux). Detection of urease activity was performed with urea agar (31) and urea-indole medium (Diagnostics Pasteur).

Nucleic acid manipulations. Genomic DNA extraction and small-scale isolation of plasmid DNA were performed as previously described (29). Large-scale plasmid DNA preparations were purified on Qiagen columns in accordance with the manufacturer's recommendations (Qiagen GmbH). Genomic and plasmid DNAs were digested with the appropriate restriction endonucleases purchased from GIBCO BRL or Promega: the resulting fragments were separated by agarose gel electrophoresis (0.8 to 1.2% agarose) and transferred onto Hybond-N^+ membranes (Amersham) by the Southern technique. Restriction fragments were eluted from agarose gels with the Qiaquick gel extraction kit (Qiagen GmbH). DNA fragments were ligated to endonuclease-restricted vectors via standard T4 DNA ligase procedures (GIBCO BRL). Recombinant plasmid DNAs were introduced into *E. coli* and *Yersinia* by transformation (29) and electroporation (7), respectively.

Prehybridization, hybridization of membrane-blotted DNA or RNA with digoxigenin-labeled DNA probes under stringent conditions, and detection of nucleic acid hybrids were all performed with the DIG hybridization and detection kit from Boehringer Mannheim.

Nucleotide sequence determination was performed by the dideoxy chain-termination method, with the ABI PRISM dichloRhodamine dye terminator sequencing kit with Amplitaq DNA polymerase FS (Perkin-Elmer), according to the manufacturer's instructions. Extension products were analyzed with the Applied Biosystems ABI 3700 automated DNA sequencer (Perkin-Elmer). Nucleotide sequences were analyzed with Perkin-Elmer software (Sequence Analysis

and Sequence Navigator). Multiple protein alignment was carried out with the CLUSTAL_X program.

PCRs. PCR amplification was performed in a 100-μl reaction volume with a thermal cycler (the 2400 model from Perkin-Elmer Cetus). Fifty nanograms of target DNA, 0.1 nmol of each primer, and 1 U of thermostable DNA polymerase were mixed in the corresponding 1× polymerase buffer (200 mM in each deoxynucleotide triphosphate). Amplification involved 30 cycles, each consisting of (i) a 1-min denaturation step at 94°C, (ii) a 1-min annealing step at 55°C, and (iii) a 1-min polymerization step at 72°C. Digoxigenin-labeled PCR products were generated with PCR DIG labeling mix from Boehringer Mannheim. Amplimers were purified on SpinX columns (Corning Costar Corporation).

Oligonucleotide primers. Nineteen primers were synthesized (by Sigma and Genset) for PCR generation of DNA fragments to be cloned or used as probes. The 5′→3′ nucleotide sequences were as follows: N1, CCCAAGCTTGAGCTC GCCTGATGCCTTTGGTGTGT; N2, TGCACTGCAGAGTGATTGCCTGT CAGGCA; N3, CGGGATCCCATTTGGGGTTAGCAATGG; N4, CCGGAA TTCGAGCTCCTGACGCAGCATTTACCATC; N5, TATCAGCCAGTGATC CAAGCA; N6, TCAACCCTACCCGTTCTGAC; N7, GCGGAATTCGAGTG AATTATTAGACCCGC; N8, GTCGAGCTCGATGCAATCCAACATATCGC; N9, GGTTGTAATACGCATGAGCC; N10, CTCAGTGAGCGAATTCAAC; N11, CGTGGTTGCTGACACTTAAG; N12, CGCCAATTATTGGCCGAT CA; N13, ATCTGGCCAATAACTGCG; K1, GCTCTGAATTCGATATCGG GGAAAGCCACGTTGTGTC; K2, GATTGGAATTCGATATCCTGAGGTC TGCCTCGTGAAGAA; C1, TCAGCGCTAGCGGAGTG; C2, GATCTGCAT CGCAGGAT; C3, TGCACTGCAGCACTCCGCTAGCGCTGA; and C4, CG GGATCCGATCTGCATCGCAGGAT.

Urease extract preparation and enzyme activity measurement. Overnight *Yersinia* cultures at 28°C in LB broth were adjusted to 10^5 cells per ml; 50 μl of bacterial culture was then added to 50 ml of fresh LB broth. *Yersinia* bacteria from a 36-h (stationary-phase) culture were harvested by centrifugation (2,600 × *g*) for 5 min at 4°C and washed twice with 0.2 M sodium phosphate buffer (pH 6.8). Bacterial cells were resuspended in phosphate buffer and disrupted twice with a French press (10,000 lb/in^2). Following centrifugation (12,800 × *g*) for 30 min at 4°C, supernatants were placed on ice. Protein concentration was determined by the Bradford dye-binding procedure according to the manufacturer's instructions (Bio-Rad). The urease activity of extracts was determined by measuring the amount of ammonia released from urea in the phenol-hypochlorite assay (20). Two micrograms of total proteins from bacterial extracts was added to 200 μl of 50 mM urea in 0.1 M sodium phosphate (pH 6.8), and the mixture was incubated at 37°C for 20 min. The reaction was stopped by addition of 400 μl of phenol-nitroprusside solution (50 g of phenol and 250 mg of sodium nitroprusside per liter). Four hundred microliters of sodium hydroxide (11 N)–sodium hypochlorite (0.175% [vol/vol]) solution was added, and the contents were mixed well. Following incubation at 50°C for 6 min, the absorbance at 625 nm was measured. A standard ammonium chloride concentration curve was determined to be linear between 28 and 448 nmol of ammonia. Absorbance values were converted to nanomoles of ammonia based on the ammonium chloride standard curve. Data are presented in terms of urease specific activity, defined as micromoles of NH_3 per minute per milligram of protein. Two micrograms of total proteins from bacterial extracts boiled for 5 min served as the negative control, and the background was subtracted from all values obtained to avoid measuring ammonia generated by urease-independent reactions.

Nickel transport. *E. coli* and *Y. pseudotuberculosis* strains were grown until the mid-exponential growth phase under microaerobic conditions in LB broth medium supplemented with molybdate and selenite, as previously described (39). The cells were washed twice and resuspended in 1 ml of transport buffer (66 mM KH_2PO_4-K_2HPO_4 [pH 6.8], 11 mM glucose, 10 mM $MgCl_2$, 0.5 mM dithionite) to a final concentration of approximately 3 to 5 mg of dry matter/ml. Solutions were purged with nitrogen and equilibrated in a 30°C water bath for 5 min.

The assay was initiated by the addition of 25 to 150 nM $^{63}NiCl_2$ (0.92 mCi μmol^{-1}; Amersham). The cation specificity was examined by using 5 μM $CdCl_2$, $CoSO_4$, $CuSO_4$, $MnSO_4$, or $ZnSO_4$ in the presence of 150 nM $^{63}NiCl_2$. Samples (0.1 ml) were taken at regular time intervals, filtered through cellulose nitrate membrane filters (Whatman; 0.45-μm pore size), and washed twice with 2 ml of rinsing buffer (66 mM KH_2PO_4-K_2HPO_4 [pH 6.8], 10 mM EDTA). Filters were placed in scintillation vials containing 5 ml of scintillation fluid (ACS; Amersham) for counting in a Packard liquid scintillation counter. Nickel uptake is expressed as picomoles of Ni^{2+} taken up per milligram (dry weight) of bacteria.

Nucleotide sequence accession number. The nucleotide sequence data reported here have been deposited in the GenBank nucleotide sequence database (accession no. AF412327 and AF412328).

RESULTS

***ureH*, encoding a putative nickel transporter, is located downstream of the *Y. pseudotuberculosis* urease locus.** We sequenced the 3′ region flanking the *ure* locus by using cosmid pMS89, which contains a ~30-kb DNA fragment encompassing the *ureABCEFGD* urease-encoding genes of *Y. pseudotuberculosis* 32777 (28). We identified a gene encoding a urea transporter (referred to as *yut*) (30) adjacent to and 378 nucleotides downstream of *ureD*, the last gene in the *ure* locus. Subsequently, we identified another gene (*ureH*, 1,059 bp) situated 148 bp downstream of *yut*: *ureH* codes for a putative 353-amino-acid protein (calculated mass, 38,693 Da) homologous to nickel permeases from *R. eutropha* (HoxN; 45 and 59% identity and similarity, respectively), *B. japonicum* (HupN; 43 and 57% identity and similarity, respectively), *M. tuberculosis* (NicT; 37 and 52% identity and similarity, respectively), and *H. pylori* (NixA; 35 and 51% identity and similarity, respectively) (Fig. 1). The similarities between the putative product of *ureH* and these proteins, together with the *ureH* gene's location close to the *Y. pseudotuberculosis ure* locus, strongly suggested that UreH is a nickel transporter. Computerized hydropathy analysis of UreH (data not shown) indicated that the protein may form eight transmembrane segments, with the carboxy- and amino-terminal regions localized in the cytoplasmic compartment—a topological feature shared by several single-peptide nickel transporters (13, 15). Four motifs which are critical for transport activity in single-component nickel permeases (13, 15) were found in UreH at positions 61 to 69, 93 to 101, 207 to 214, and 244 to 252, respectively (Fig. 1).

Inactivation of the *ureH* gene does not abolish urease activity in *Y. pseudotuberculosis*. To test whether the UreH nickel carrier is essential for urease activity in *Y. pseudotuberculosis*, a *ureH* mutant (MYUH) was made in wild-type strain 32777. A 1,093-bp intragenic deletion was replaced by a kanamycin resistance cassette. This was introduced by allelic exchange after mating *Y. pseudotuberculosis* strain 32777 with *E. coli* strain SM10 λ*pir* harboring the pFSΔU plasmid (Table 1). The MYUH *ureH* mutant was selected on sucrose agar (3). Its genotype was confirmed by PCR assays with primer sets N11-K2 and N12-K1 and by Southern blot hybridization with two appropriate DNA probes, one corresponding to the *kan* cassette and the other corresponding to the upstream region of *ureH* (Fig. 2).

The ability of the MYUH mutant to degrade urea was tested in bacteria cultured in LB broth. Surprisingly, no significant difference in ureolytic activity was found compared with the wild-type strain. Enzyme activity was determined by using media with limiting and high nickel ion concentrations in order to account for the possibility that UreH functionality might be metal dose dependent. No difference (variance analysis: F test, $P > 0.05$) between the wild-type and *ureH* mutant strains was detected after growth of bacteria in LB broth containing increasing amounts of either the nickel chelator nitrilotriacetic acid or nickel chloride (Fig. 3). Furthermore, urease activity of the mutant was similar to that of the parent (data not shown) when the bacteria were cultured in the presence of 100 mM $MgCl_2$, which inhibits nonspecific, divalent cation transporters (11) that could otherwise impede detection of nickel transport by UreH.

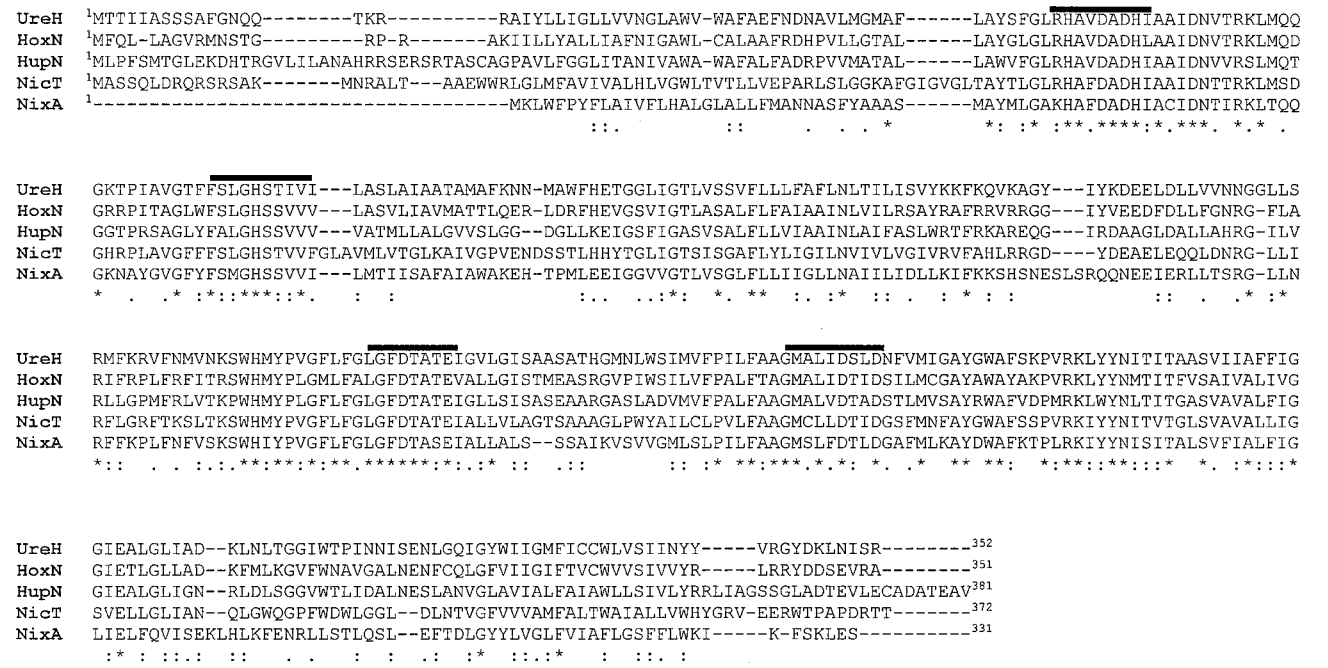

FIG. 1. Alignment of the amino acid sequence of the UreH protein from *Y. pseudotuberculosis* 32777 with those of nickel transporters from *R. eutropha* (HoxN), *B. japonicum* (HupN), *M. tuberculosis* (NicT), and *H. pylori* (NixA). Asterisks, colons, and periods indicate identical, similar, and related amino acids, respectively. Dashes correspond to gaps introduced to optimize homology between sequences. Motifs critical for biological activity are overlined.

Nickel uptake is restored in an *E. coli nikA* mutant *trans*-complemented with the *Y. pseudotuberculosis ureH* gene. Although no defect in ureolytic activity could be observed in the *ureH* mutant, UreH was shown to behave as a nickel carrier by heterologous complementation of an *E. coli* nickel transporter-deficient *nikA* mutant (HPX72) with the *Y. pseudotuberculosis ureH* gene. Like almost all *E. coli* strains, strain HPX72 is nonureolytic. When this strain was cotransformed with compatible plasmids pFS45 bearing the *ureH* gene and pFS50 harboring the *Y. pseudotuberculosis ure* locus with its promoter region, it was able to degrade urea. As a control, strain HPX72 containing pFS50 alone was nonureolytic. The presence of the *ureH* gene restored hydrogenase activity to the same level as that of the *E. coli* wild-type strain P4X (data not shown). Therefore, the *Y. pseudotuberculosis ureH* gene appears to be able to functionally replace the *E. coli nik* locus, thus allowing production of active urease and hydrogenase. Secondly, nickel uptake assays were performed in order to substantiate the role of UreH in nickel transport. Assays were conducted in the presence of 10 mM $MgCl_2$ and at low nickel concentrations (150 nM). Introduction of plasmid pFS45 restored HPX72's rate of nickel transport to a level similar to that obtained by homologous complementation of the mutant with pLW21 bearing the entire *E. coli nik* locus (Fig. 4A).

The 5′ end of the *Y. pseudotuberculosis* urease locus is flanked by the Ynt ABC-nickel transport system. Since urease activity in *Y. pseudotuberculosis* was not impaired by *ureH* inactivation, we suspected the existence of another nickel carrier in this bacterium. Sequencing of the 5-kb DNA region upstream of *ureA* allowed identification of five open reading frames (ORFs). ORF1 (1,578 bp), ORF2 (969 bp), ORF3 (807 bp), ORF4 (807 bp), and ORF5 (666 bp) are apparently arranged in an operon-like manner since (i) all are transcribed in the same direction and (ii) intergenic spaces between neighboring ORFs vary between −1 and −8 nucleotides. ORF5 was situated 1,198 bp from *ureA*, the first gene of the *ure* locus. The putative proteins encoded by these five ORFs show striking amino acid sequence similarities to components of the *E. coli* Nik specific nickel ABC transport system—between 25 and 32% identity, depending on the operon component in question (24). ORF1 encodes a 525-amino-acid protein (predicted molecular mass of 57,820 Da) which is homologous to the *E. coli* NikA periplasmic nickel-binding protein. The putative ORF2 and ORF3 polypeptides (322 and 268 amino acids with calculated molecular masses of 35,233 and 30,002 Da, respectively) were predicted to contain six potential transmembrane domains, displaying similarity to the NikB and NikC integral cytoplasmic membrane proteins. Like NikD and NikE, ORF4 (268 amino acids, molecular mass of 29,472 Da) and ORF5 (221 amino acids, molecular mass of 24,754 Da) possess characteristic ATP-binding domains (37), suggesting a role in coupling energy to the transport process. ORF1 to ORF5 also showed homology to the *nikABCDE* cluster of *B. suis* (24 to 32% identity) (18) and that of *V. parahaemolyticus* (33 to 41% identity) (26). They also share 34 to 43% identity with the dipeptide transport system encoded by the *dpp* operon from *Streptococcus pyogenes* (27). Furthermore, the *Y. pseudotuberculosis* gene cluster exhibits the highest homology of all (51 to 72% identity) with the *oxd-6* operon from *Salmonella enterica* serovar Typhimurium: it has been supposed that this operon encodes a nickel or peptide transporter (38), but the matter has yet not been clearly resolved. Finally, the putative ORF1

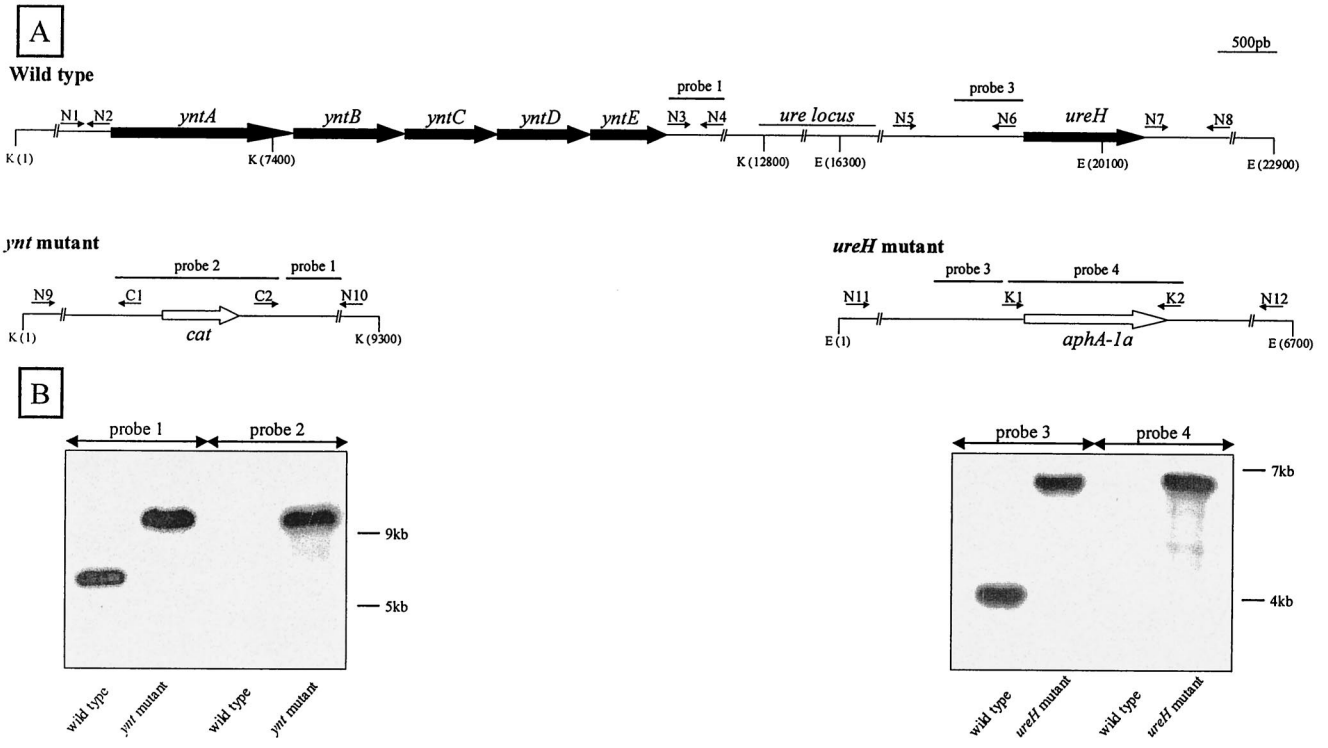

FIG. 2. Genetic organization of the immediate environment of the chromosomal urease (*ure*) locus and genotype analysis of *ynt*- and *ureH*-deficient mutants of *Y. pseudotuberculosis* 32777. (A) *Kpn*I (K) and *Eco*RI (E) restriction map of the chromosome of wild-type strain 32777 and isogenic mutants MYUH (*ureH*) and MYNT (*ynt*). (B) (Left) Southern blot of *Kpn*I-digested DNA from wild-type strain 32777 and the *yntABCDE*-deficient mutant hybridized with probe 1 (0.5 kb, corresponding to the downstream region of *yntE*) and probe 2 (1.4 kb, detecting the chloramphenicol resistance gene *cat*). (Right) Southern blot of *Eco*RI-digested DNA from wild-type strain 32777 and the *ureH*-deficient mutant hybridized with probe 3 (0.6 kb, corresponding to the upstream region of *ureH)* and probe 4 (1.3 kb, detecting the kanamycin resistance gene *aphA-1a*). Primers N1 to N12, K1, K2, C1, and C2 were used both for creating mutants and for checking their genotype. Numbers in parentheses indicate the DNA sequence coordinates.

product was found to be 70% identical to that of an unidentified ORF (also referred to as Orf-1) which follows the regulatory *ureR* gene present on a 160-kb plasmid in a urease-producing, pathogenic *E. coli* strain (10). On the whole, these features suggest that the five ORFs code for a nickel transport system, and we thus named them *yntA* (for *Yersinia* nickel transport), *yntB*, *yntC*, *yntD*, and *yntE*, respectively. To prove that they were involved in Ni^{2+} uptake, we used the same approach as for the *ureH* gene. When plasmid pFS78 bearing the *yntABCDE* operon was introduced into the *E. coli nikA* mutant HPX72 harboring the *Y. pseudotuberculosis* urease cluster borne on plasmid pFS50, ureolytic capacity was restored. In addition, nickel uptake was mediated by the Ynt system at a higher initial rate than that by the UreH system or the *E. coli* Nik transporter (Fig. 4A).

The Ynt transport system is essential for urease activation in *Y. pseudotuberculosis*. To assess the physiological role of the Ynt system in *Y. pseudotuberculosis*, a *ynt*-deficient mutant was constructed from wild-type strain 32777, as for the MYUH mutant. Complete deletion of the *ynt* operon was obtained by using plasmid pFSΔO (Table 1). The genotype of the resulting *ynt* mutant MYNT was confirmed by PCR assays with the primer sets N9-C1 and N10-C2 and by Southern blot hybridization with appropriate DNA probes (Fig. 2). After growth in LB broth, the *ynt* mutant's urease activity was dramatically reduced (by 99%) compared with that of the wild-type strain (0.050 ± 0.001 versus 4.8 ± 0.5 μM NH_3/min/mg of protein; Student's *t* test, $P < 0.05$) and was completely abolished by concomitant inactivation of *ureH* (≤0.01 μM NH_3/min/mg of protein). These data indicate that, in contrast to the *ureH* gene, the *ynt* genes play a major role for urease activation in *Y. pseudotuberculosis*.

Both Ynt and UreH are nickel-specific transporters. To determine the respective contribution of each *Y. pseudotuberculosis* nickel transporter, the ability of the single or double *ureH* and *ynt* mutants to take up nickel was compared with that of the parental strain (Fig. 4B). Accumulation of nickel by the MYOU double mutant was below the threshold of the assay. Uptake in the single mutants MYUH and MYNT can therefore be ascribed to nickel transport by the sole remaining transport system present in these strains. Time course experiments demonstrated that the MYUH mutant's Ynt system gave a significantly (variance analysis: F test, $P < 10^{-3}$) higher rate of uptake than did the MYNT mutant's UreH transporter.

To test the specificity of Ynt and UreH, the effects of cadmium, cobalt, copper, manganese, and zinc ions on nickel uptake by each nickel transporter-deficient *Y. pseudotuberculosis* mutant were investigated. The competing metal ions were added to a final concentration ~30-fold greater than that of Ni^{2+} ions (i.e., 5 μM versus 150 nM). None of the metal ions

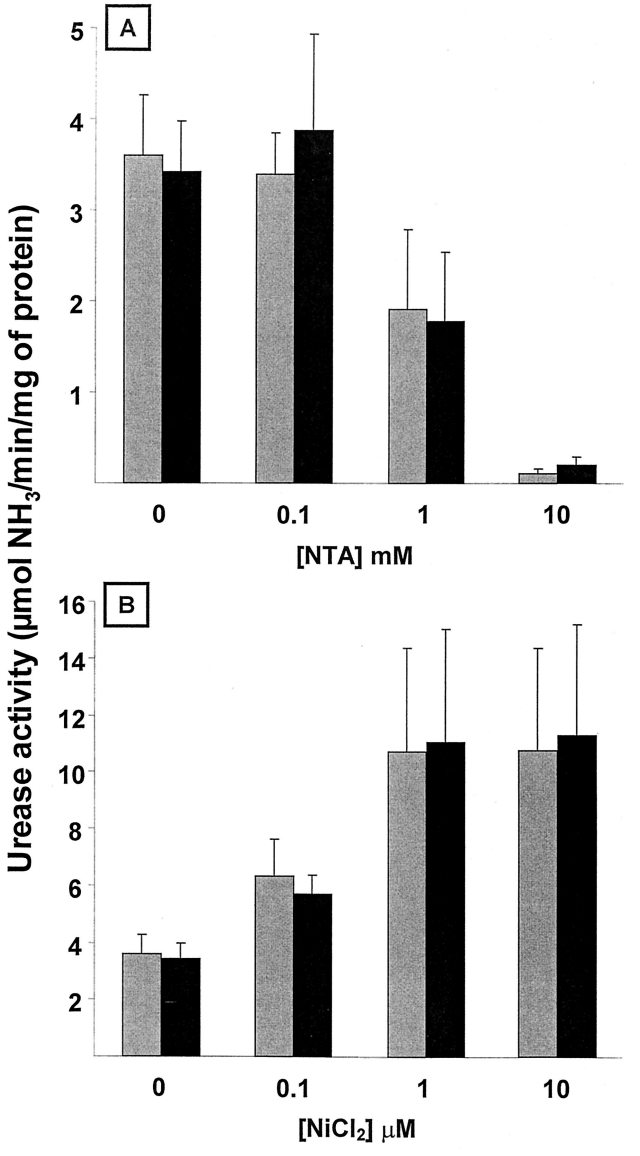

FIG. 3. Ureolytic activity of wild-type strain 32777 (gray bars) and the MYUH *ureH* mutant (black bars) following growth in LB broth containing increasing concentrations of the nickel chelator nitrilotriacetic acid (NTA) (A) or $NiCl_2$ (B). Each bar is the mean value of three independent experiments ± the standard deviation.

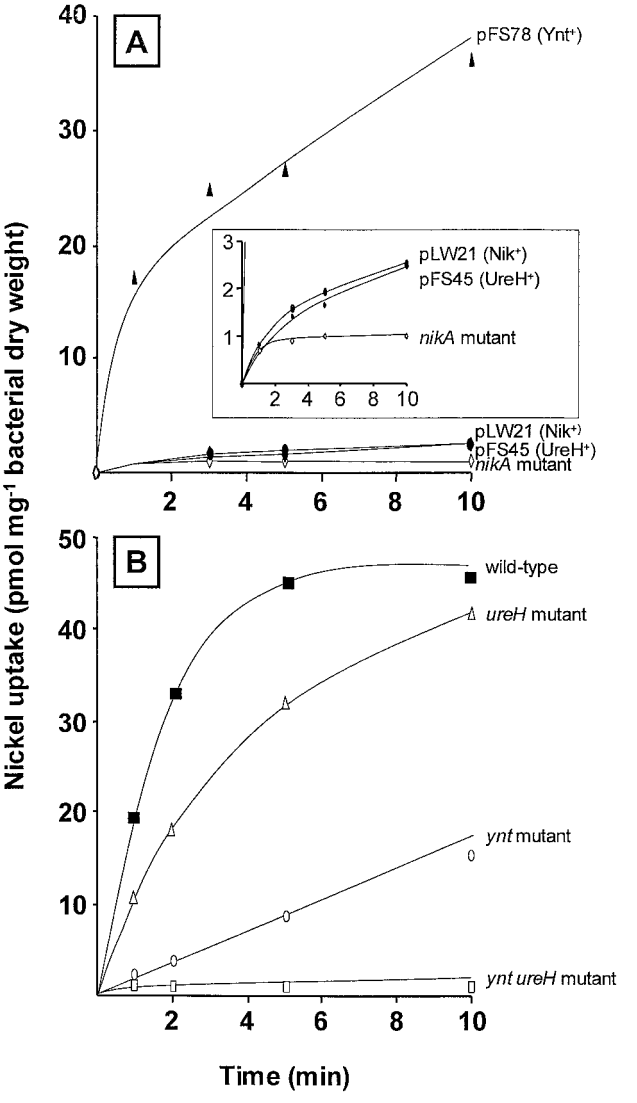

FIG. 4. Roles of UreH and Ynt in nickel entry into bacteria. Bacterial suspensions were incubated in the presence of 150 nM $^{63}NiCl_2$ and 10 mM $MgCl_2$. Nickel uptake was assessed at regular intervals. Three separate experiments gave similar results. Representative data are shown. (A) Nickel uptake into *nikA*-deficient *E. coli* strain *trans*-complemented with *ureH* (pFS45) or *yntABCDE* (pFS78) genes from *Y. pseudotuberculosis* and *nikABCDE* genes (pLW21) from *E. coli*. (B) Nickel uptake into *Y. pseudotuberculosis ureH*, *yntABCDE*, and *ureH yntABCDE* mutants derived from the wild-type strain.

caused significant inhibition of nickel entry into either of the mutants (data not shown). Finally, to estimate the affinity of each transporter for Ni^{2+} ions, transport assays were conducted by using $NiCl_2$ concentrations ranging from 25 to 150 nM. The K_T value of each transporter was estimated from the initial (linear) uptake rates (<2 min) at 50 ± 5 nM (mean value ± standard deviation of two independent determinations) for UreH and 70 ± 15 nM for Ynt.

DISCUSSION

Nickel transporters play a critical role in the biosynthesis of nickel-dependent enzymes such as hydrogenases and ureases (12). For the first time, we demonstrate the presence of two transporters specific for nickel in a prokaryote. The human and animal pathogen *Y. pseudotuberculosis* possesses (i) an ABC transporter encoded by the *yntABCDE* gene cluster, which shows some degree of similarity to the Nik system in several gram-negative bacteria (2, 18, 24, 26), and (ii) a single-component carrier encoded by the *ureH* gene, displaying homology to polypeptides of the nickel-cobalt transporter family exemplified by HoxN (13). Complete suppression of nickel transport in the *ynt ureH* double mutant indicated that, apart from Ynt and UreH, there are no other Ni^{2+}-specific transport systems in *Y. pseudotuberculosis*. *H. pylori* also has two transport systems for nickel acquisition: the high-affinity nickel carrier protein NixA

(22) and an ABC transporter (17). However, the latter has not been proven to be specific for nickel.

Database searches revealed that genes homologous to *ureH* and *ynt* are present in the genome of the other two pathogenic *Yersinia* species, *Y. pestis* (designated by "p") and *Y. enterocolitica* (designated by "ent"). Deduced amino acid sequences from $ureH_p$ and $ureH_{ent}$ are 99 and 93% identical, respectively, to that of the *ureH* product from *Y. pseudotuberculosis*, whereas putative Ynt_p and Ynt_{ent} complexes share 99 and 91.6% of residues, respectively, with Ynt proteins from *Y. pseudotuberculosis*. Phylogenetic analysis of the putative periplasmic nickel-binding protein encoded by the *yntA* gene from these three pathogenic *Yersinia* species showed that YntA, $YntA_p$, and $YntA_{ent}$ cluster with the serovar Typhimurium nickel-binding-protein-related Oxd-6a polypeptide and also with the *orf1* gene product from urease-producing *E. coli* strains. Hence, besides the Nik transport system group, the bacterial nickel-ABC transporter family includes another subclass, with Ynt as a prototype carrier and two other members produced by *Salmonella* and some *E. coli* isolates.

For several bacterial species in which nickel-transport systems were characterized, genes specifying these carriers were found within or in proximity to genetic loci encoding the nickel-requiring enzyme urease (1, 2, 19, 26) or hydrogenase (13). In addition, nickel permeases of the ABC family are encoded by gene clusters which are harbored either on a plasmid (10), on a pathogenicity island (26), or adjacent to an insertion sequence (2, 26). In *Y. pseudotuberculosis*, *ureH* flanks the *yut* gene (30), located just downstream of the urease accessory gene *ureD*, whereas the *yntABCDE* polycistronic unit is upstream of the *ureA* structural urease gene. The fact that the intergenic space (1,198 bp) between *yntE* and *ureA* has a low G+C content (34 versus 47% for the whole *Y. pseudotuberculosis* genome) and includes many repeated sequences is noteworthy. Furthermore, a copy of insertion sequence IS*285* is present 1,848 bp upstream of the *Y. pestis yntA* gene. Taken together, these genetic features suggest that the chromosomal region containing the *ynt* operon has been the site of DNA recombination events and that the nickel ABC transport system could have been acquired by yersiniae through horizontal gene transfer.

Nickel uptake assays with *Y. pseudotuberculosis ureH* and *ynt* mutants revealed that cellular entry of this divalent cation occurs principally via the Ynt ABC transporter. At the nickel concentration used for the assay, initial rates of nickel uptake by *ynt* and *ureH* mutants reached approximately 15 and 60%, respectively, of the wild-type value (Fig. 4B), although the K_T values of UreH and Ynt are similar. This discrepancy could be due to better production of Ynt under our in vitro bacterial growth conditions. Surprisingly, urease activity was not found to correlate with nickel accumulation inside the cells, since it was shown to be strongly reduced (99%) after *ynt* inactivation but did not significantly differ from that of wild-type *Y. pseudotuberculosis* after *ureH* knockout, regardless of nickel or magnesium concentrations in the growth medium. This was not due to a polar effect of the *ynt* mutation on the downstream *ure* locus, since urease activity of the *ynt* mutant was fully restored after *trans*-complementation with the *ynt* operon. These discrepancies between the mutants' ureolytic and nickel uptake capacities could be due to regulation by nickel concentration of the *Y. pseudotuberculosis* urease gene cluster expression, as has been recently demonstrated for *H. pylori* urease, which is induced by Ni^{2+} at the transcriptional level (35). Mutation of *ynt* would thus reduce the intracellular nickel concentration below the threshold necessary for induction.

Although weakly homologous (between 25 and 32% identity) to *E. coli* Nik permease, the *Y. pseudotuberculosis* Ynt complex is functionally interchangeable with this ABC transporter. However, *E. coli* cells incorporated much more nickel when expressing *ynt* instead of the *nik* gene cluster (Fig. 4A). In the same heterogenous genetic background, UreH is also functional and is as efficient as the endogenous Nik transport system (Fig. 4A). The differences in these systems' nickel transport capacities may reside in their expression in *E. coli* and could also be linked to their conformation in the cell membrane.

The production of redundant nickel-specific permeases by yersiniae emphasizes the importance of the penetration of this divalent cation into the cell in relation to the biosynthesis of urease—and possibly that of other nickel-dependent enzymes. It also poses the question of their physiological role and raises the possibility that the two systems are expressed under different growth conditions at various stages of the life cycle.

ACKNOWLEDGMENTS

F. Sebbane received a doctoral studentship from the Ministère de l'Enseignement Supérieur, de la Recherche et de la Technologie and from the Fondation pour la Recherche Médicale. This work was supported in part by the European Regional Development Fund (to M.S.) and by a grant from the Programme de Recherche Fondamentale en Microbiologie et Maladies Infectieuses et Parasitaires from the Ministère de la Recherche (to M.-A.M.-B.).

We thank P. Vincent for assistance in statistical analysis.

REFERENCES

1. **Beckwith, C. S., D. J. McGee, H. L. Mobley, and L. K. Riley.** 2001. Cloning, expression, and catalytic activity of *Helicobacter hepaticus* urease. Infect. Immun. **69:**5914–5920.
2. **Bosse, J. T., H. D. Gilmour, and J. I. MacInnes.** 2001. Novel genes affecting urease activity in *Actinobacillus pleuropneumoniae*. J. Bacteriol. **183:**1242–1247.
3. **Carnoy, C., C. Mullet, H. Müller-Alouf, E. Leteurtre, and M. Simonet.** 2000. Superantigen YPMa exacerbates the virulence of *Yersinia pseudotuberculosis* in mice. Infect. Immun. **68:**2553–2559.
4. **Chang, A. C., and S. N. Cohen.** 1978. Construction and characterization of amplifiable multicopy DNA cloning vehicles derived from the P15A cryptic miniplasmid. J. Bacteriol. **134:**1141–1156.
5. **Chivers, P. T., and R. T. Sauer.** 2000. Regulation of high affinity nickel uptake in bacteria. Ni^{2+}-dependent interaction of NikR with wild-type and mutant operator sites. J. Biol. Chem. **275:**19735–19741.
6. **Cole, S. T., R. Brosch, J. Parkhill, T. Garnier, C. Churcher, D. Harris, S. V. Gordon, K. Eiglmeier, S. Gas, C. E. Barry III, F. Tekaia, K. Badcock, D. Basham, D. Brown, T. Chillingworth, R. Connor, R. Davies, K. Devlin, T. Feltwell, S. Gentles, N. Hamlin, S. Holroyd, T. Hornsby, K. Jagels, B. G. Barrell, et al.** 1998. Deciphering the biology of *Mycobacterium tuberculosis* from the complete genome sequence. Nature **393:**537–544.
7. **Conchas, R. F., and E. Carniel.** 1990. A highly efficient electroporation system for transformation of *Yersinia*. Gene **87:**133–137.
8. **De Pina, K., V. Desjardin, M. A. Mandrand-Berthelot, G. Giordano, and L. F. Wu.** 1999. Isolation and characterization of the *nikR* gene encoding a nickel-responsive regulator in *Escherichia coli*. J. Bacteriol. **181:**670–674.
9. **Donnenberg, M. S., and J. B. Kaper.** 1991. Construction of an *eae* deletion mutant of enteropathogenic *Escherichia coli* by using a positive-selection suicide vector. Infect. Immun. **59:**4310–4317.
10. **D'Orazio, S. E., V. Thomas, and C. M. Collins.** 1996. Activation of transcription at divergent urea-dependent promoters by the urease gene regulator UreR. Mol. Microbiol. **21:**643–655.
11. **Eitinger, T., O. Degen, U. Bohnke, and M. Muller.** 2000. Nic1p, a relative of bacterial transition metal permeases in *Schizosaccharomyces pombe*, provides nickel ion for urease biosynthesis. J. Biol. Chem. **275:**18029–18033.
12. **Eitinger, T., and M. A. Mandrand-Berthelot.** 2000. Nickel transport systems in microorganisms. Arch. Microbiol. **173:**1–9.

13. **Eitinger, T., L. Wolfram, O. Degen, and C. Anthon.** 1997. A Ni^{2+} binding motif is the basis of high affinity transport of the *Alcaligenes eutrophus* nickel permease. J. Biol. Chem. **272:**17139–17144.
14. **Fu, C., S. Javedan, F. Moshiri, and R. J. Maier.** 1994. Bacterial genes involved in incorporation of nickel into a hydrogenase enzyme. Proc. Natl. Acad. Sci. USA **91:**5099–5103.
15. **Fulkerson, J. F., Jr., and H. L. Mobley.** 2000. Membrane topology of the NixA nickel transporter of *Helicobacter pylori*: two nickel transport-specific motifs within transmembrane helices II and III. J. Bacteriol. **182:**1722–1730.
16. **Hanahan, D.** 1983. Studies on transformation of *Escherichia coli* with plasmids. J. Mol. Biol. **166:**557–580.
17. **Hendricks, J. K., and H. L. Mobley.** 1997. *Helicobacter pylori* ABC transporter: effect of allelic exchange mutagenesis on urease activity. J. Bacteriol. **179:**5892–5902.
18. **Jubier-Maurin, V., A. Rodrigue, S. Ouahrani-Bettache, M. Layssac, M. A. Mandrand-Berthelot, S. Kohler, and J. P. Liautard.** 2001. Identification of the *nik* gene cluster of *Brucella suis*: regulation and contribution to urease activity. J. Bacteriol. **183:**426–434.
19. **Maeda, M., M. Hidaka, A. Nakamura, H. Masaki, and T. Uozumi.** 1994. Cloning, sequencing, and expression of thermophilic *Bacillus* sp. strain TB-90 urease gene complex in *Escherichia coli*. J. Bacteriol. **176:**432–442.
20. **McGee, D. J., C. A. May, R. M. Garner, J. M. Himpsl, and H. L. Mobley.** 1999. Isolation of *Helicobacter pylori* genes that modulate urease activity. J. Bacteriol. **181:**2477–2484.
21. **Miller, V. L., and J. J. Mekalanos.** 1988. A novel suicide vector and its use in construction of insertion mutations: osmoregulation of outer membrane proteins and virulence determinants in *Vibrio cholerae* requires *toxR*. J. Bacteriol. **170:**2575–2583.
22. **Mobley, H. L., R. M. Garner, and P. Bauerfeind.** 1995. *Helicobacter pylori* nickel-transport gene *nixA*: synthesis of catalytically active urease in *Escherichia coli* independent of growth conditions. Mol. Microbiol. **16:**97–109.
23. **Mobley, H. L., M. D. Island, and R. P. Hausinger.** 1995. Molecular biology of microbial ureases. Microbiol. Rev. **59:**451–480.
24. **Navarro, C., L. F. Wu, and M. A. Mandrand-Berthelot.** 1993. The *nik* operon of *Escherichia coli* encodes a periplasmic binding-protein-dependent transport system for nickel. Mol. Microbiol. **9:**1181–1191.
25. **Nikaido, H.** 1994. Porins and specific diffusion channels in bacterial outer membranes. J. Biol. Chem. **269:**3905–3908.
26. **Park, K. S., T. Iida, Y. Yamaichi, T. Oyagi, K. Yamamoto, and T. Honda.** 2000. Genetic characterization of DNA region containing the *trh* and *ure* genes of *Vibrio parahaemolyticus*. Infect. Immun. **68:**5742–5748.
27. **Podbielski, A., and B. A. Leonard.** 1998. The group A streptococcal dipeptide permease (Dpp) is involved in the uptake of essential amino acids and affects the expression of cysteine protease. Mol. Microbiol. **28:**1323–1334.
28. **Riot, B., P. Berche, and M. Simonet.** 1997. Urease is not involved in the virulence of *Yersinia pseudotuberculosis* in mice. Infect. Immun. **65:**1985–1990.
29. **Sambrook, J., and D. W. Russell.** 2001. Molecular cloning: a laboratory manual, 3rd ed. Cold Spring Harbor Laboratory Press, Cold Spring Harbor, N.Y.
30. **Sebbane, F., S. Bury-Moné, K. Cailliau, E. Browaeys-Poly, H. De Reuse, and M. Simonet.** 2002. The *Yersinia pseudotuberculosis* Yut protein, a new type of urea transporter homologous to eukaryotic channels and functionally interchangeable *in vitro* with the *Helicobacter pylori* UreI protein. Mol. Microbiol. **45:**1165–1174.
31. **Sebbane, F., A. Devalckenaere, J. Foulon, E. Carniel, and M. Simonet.** 2001. Silencing and reactivation of urease in *Yersinia pestis* is determined by one G residue at a specific position in the *ureD* gene. Infect. Immun. **69:**170–176.
32. **Simon, R., U. Priefer, and A. Puhler.** 1983. A broad host range mobilization system for in vitro genetic engineering: transposon mutagenesis in Gram negative bacteria. Bio/Technology **1:**784–791.
33. **Smith, R. L., M. A. Szegedy, L. M. Kucharski, C. Walker, R. M. Wiet, A. Redpath, M. T. Kaczmarek, and M. E. Maguire.** 1998. The CorA Mg^{2+} transport protein of *Salmonella typhimurium*. Mutagenesis of conserved residues in the third membrane domain identifies a Mg^{2+} pore. J. Biol. Chem. **273:**28663–28669.
34. **Taylor, L. A., and R. E. Rose.** 1988. A correction in the nucleotide sequence of the Tn*903* kanamycin resistance determinant in pUC4K. Nucleic Acids Res. **16:**358.
35. **van Vliet, A. H., E. J. Kuipers, B. Waidner, B. J. Davies, N. de Vries, C. W. Penn, C. M. Vandenbroucke-Grauls, M. Kist, S. Bereswill, and J. G. Kusters.** 2001. Nickel-responsive induction of urease expression in *Helicobacter pylori* is mediated at the transcriptional level. Infect. Immun. **69:**4891–4897.
36. **Vieira, J., and J. Messing.** 1982. The pUC plasmids, an M13mp7-derived system for insertion mutagenesis and sequencing with synthetic universal primers. Gene **19:**259–268.
37. **Walker, J. E., A. Eberle, N. J. Gay, M. J. Runswick, and M. Saraste.** 1982. Conservation of structure in proton-translocating ATPases of *Escherichia coli* and mitochondria. Biochem. Soc. Trans. **10:**203–206.
38. **Wei, Y., and C. G. Miller.** 1999. Characterization of a group of anaerobically induced, *fnr*-dependent genes of *Salmonella typhimurium*. J. Bacteriol. **181:**6092–6097.
39. **Wu, L. F., and M. A. Mandrand-Berthelot.** 1986. Genetic and physiological characterization of new *Escherichia coli* mutants impaired in hydrogenase activity. Biochimie **68:**167–179.